HiSST: 3rd International Conference on
High-Speed Vehicle Science Technology
14 -19 April 2024, Busan, Korea

Fluid-thermal-structural coupled study on rudder leading edge with porous opposing jet in hypersonic flows

Shaliang Li [1], Bing Liu, Shibin Li, Wei Huang, Lin Wang

Abstract

Hypersonic air rudders face extreme force/thermal environments, and opposing jet can improve the thermal environment in their stationing or leading edge regions. In order to understand the effects and mechanisms of porous opposing jet at rudder leading edges, a numerical simulation study is carried out, by using a two-way loose coupling method of fluid-thermal-structural. The drag reduction and heat prevention mechanisms of no jet and porous jet is comprehensively compared and analyzed. The results show that the introduction of the porous opposing jet change flow field at the leading edge of the air rudder, the bow shock is pushed outward, and its surge surface shows regular undulations. The porous opposing jet can provide a good effect in both drag reduction and thermal protection, which reduces the overall temperature of the rudder leading edge by about 20% and the heat flux by about 25%.

Keywords: *hypersonic vehicle, opposing jet, fluid-thermal-structural coupling, drag reduction, thermal protection*

Nomenclature

Latin
Ma – Mach number
R – radius
d – diameter
G – shear moduli
E – Young's moduli
PR - jet pressure ratio
H – flight hight
q_w – wall heat flux
T_w – wall temperature
t_0 – initial time
Δt – time step
P – pressure
P_0 – stagnation pressure
T – temperature
Re – Renolds number
Pr – Prandtl number
St – Stanton number
T_{aw} – wall recovery temperature
Greek
ρ – density
C_P – specific heat
λ – thermal conductivity
α – coefficients of thermal expansion
γ – specific heat
Subscripts
∞ – free stream
j – opposing jet

1. Introduction

Hypersonic vehicles have great application value and potential economic value, due to its advantages of fast speed, great penetrating capability and remarkable stealth effect. With the progress of science and technology, countries have put forward higher requirements on the strike range and maneuverability of hypersonic vehicles, and the vehicles design and research for wide-speed range and large airspace have become one of the hottest spots[1-3].

[1] *Hypersonic Technology Laboratory, College of Aerospace Science and Engineering, National University of Defense Technology, Changsha, Hunan, 410073, People's Republic of China, lishaliang@nudt.edu.cn*
Corresponding author *Hypersonic Technology Laboratory, College of Aerospace Science and Engineering, National University of Defense Technology, Changsha, Hunan, 410073, People's Republic of China, wanglin07@nudt.edu.cn*

Due to air stagnation and skin friction, hypersonic vehicles face extreme force/heat loads during flight, especially in critical areas such as air rudders/wings. Under complex incoming flow, the strong interaction between flow field and structure of vehicles generates strong coupling problems among aerodynamic, heating and structure. The traditional structural design of thermal protection can no longer meet the new requirements, which brings a great challenge to aerodynamic configuration and structural design of vehicles. Active cooling techniques, such as opposing jet[4-6], have been proposed to improve the thermal environment in stationary point and leading edge through active flow control.

But most of previous studies on related problems was based on uncoupled approach, assuming isothermal-wall condition on the solid surface. Compared to coupled strategy, the main problem brought by simplification is the overestimation of aerodynamic heating, which is unfavorable for accurate study of heating effects. In addition, the corresponding structural response also needs to be investigated. Hence, a coupled analysis is necessary to safeguard flight performance of hypersonic vehicles.

On the basis of single opposing jet, Fan and Li[7-9] presented the application of porous opposing jet technology to blunt hypersonic vehicle. Liu[10] numerically investigated the heat transfer characteristics of the blunt leading edge with opposing jet by fluid-thermal coupled method. Then, Liu[11] found that a suitable *PR* should be selected to balance the drag reduction and thermal protection effect with the stress effect of the jet on the head. Meng[12] demonstrated that the porous jet is more benefit to drag and heat reduction of high-speed vehicle than the single-hole jet. When the porous jet strategy is used, the lift-drag ratio is increased by 4.23%, and the total heat flux at the characteristic centerline of jet holes is significantly reduced to 108 kW/m^2.

Zhu[13] proposed a novel combinational spike-aerodome and lateral jet, and thoroughly investigated the effects of *PR*, length of the spike, and diameter of the aerodome on high-speed flow characteristics and thermal response. On this basis, Meng[14-16] adopted a combination strategy of spike and multiple jet, and further explored the effects of lateral jet position on pressure and thermal flow. Subsequently, this combination scheme was also applied to waverider. The effects of different combinations and angles of attack on the flow field and aerodynamic characteristics were investigated.

However, the thermal response and structural response under porous opposing jet remain unclear, and the mechanisms of fluid-thermal-structural coupling and thermal protection also need to be studied. Hence, the fluid-thermal-structural coupling method is adopted to study the hypersonic air rudders with porous opposing jet, and to understand the fluid-thermal-structural coupling mechanism of air rudders under complex flows. It provides a solution for structural deformation of the rudders in extreme force/heat environments, and it is of great reference significance for the overall design of air rudders.

2. Physical model and numerical methodology

2.1. Physical model

The schematic diagram of the air rudder is shown in Fig 1, the radius of the leading edge is set R as 5mm, the swept angle is 30°, the height is 200 mm, and the wall thickness is 1 mm. 7 jet holes are distributed longitudinally in the leading edge of the rudder, the diameter of the jet d is 1 mm, and the spacing among the orifices is 30 mm. The characteristic line A is taken along the centerline of the leading edge, and the line B is taken along the central jet hole. The origin of the coordinate axis is the curvature center of leading edge in the rudder bottom surface

The air rudder is assumed to work at flight conditions of Ma = 6, H = 25km. The pressure ratio (PR) of the jet is set to 0.4, which is defined as the total pressure ratio of the opposing jet to the free stream. The opposing jet is perpendicular to the jet exit plane, with temperature of 300 K and Mach number of 1.0. The initial temperature of the coupling wall is 300 K. The coupling time step Δt is 0.001 s. The grid is shown in Fig 2, and the smallest height of boundary-layer grid on the coupling surface is 1×10^{-6} m. The grid boundary layer is locally refined. AISI 304 stainless steel is chosen as the air rudder material, and its material properties are shown in Table 1.

Table 1. Material properties of AISI 304

P (kg/m3)	C_P (J/kg·K)	λ (W/m·K)	α (10^{-6} /K)	E (Gpa)	G (Gpa)
7850	500	16.2	17.3	200	73.7

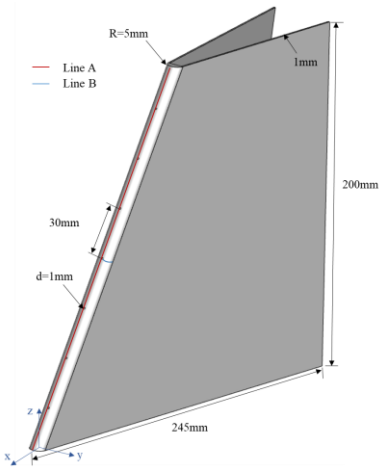

Fig 1. Physical model

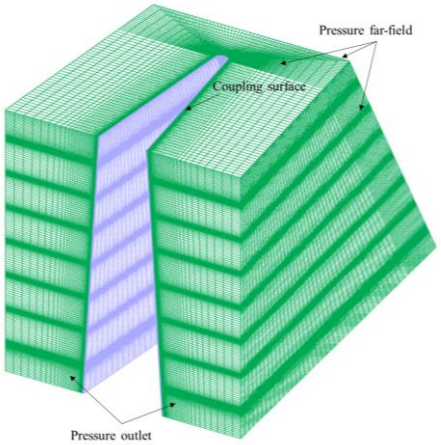

Fig 2. Computational grids

2.2. Numerical method

The three-dimensional Reynolds-Average Navier-Stokes (RANS) equations for unsteady compressible flow are used as the governing equations. The convective terms are approximated by the AUSM+ scheme, the MUSCL method is used to improve the numerical accuracy. The SST k-ω turbulence model is selected to capture the flow field characteristics.

For solid domain, the unsteady temperature field of structure caused by aeroheating is modeled by solving Fourier heat conduction. The effect of wall radiation is neglected here. Under the influence of aerodynamic forces and heat flow, the governing equations for thermoselasticity of three dimensional model are compatibility equation of strains, Cauchy's relationship between traction and stress, and the stress equilibrium equations in Cartesian coordinates. The solid part is regarded as an isotropic linear thermoelastic body.

For hypersonic multi-physics interaction problems, the characteristic time of the fluid response is smaller than the structural thermal response by 3-4 orders of magnitude most of the time. Therefore, it can be assumed that the change in flow field properties is small during the characteristic time of structural thermal response. In order to reduce computing time and improve computational efficiency, the loose coupling strategy is proposed, which takes the characteristic time of structural thermal response as the time step of coupling iteration.

The bidirectional coupling and unidirectional coupling are combined together for the loose coupling analysis. Fig 1 shows the complete coupling strategy. Specifically, it can be summarized as:

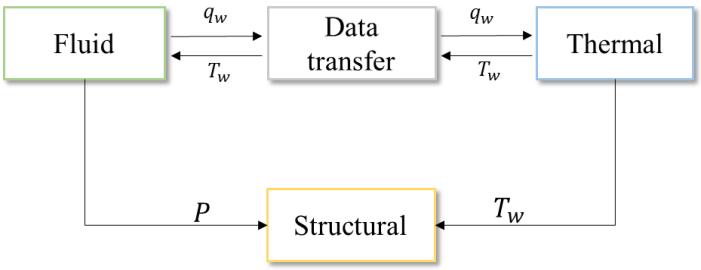

Fig 1. Graphical representation of coupling techniques

1) At the initial time t_0, the solid domain is given an initial constant temperature as the initial boundary condition for flow field calculation.
2) Calculate the flow field using the given boundary conditions to obtain the heat flux distribution.
3) Transferring heat flux distribution of coupled surface to the solid domain, the transient heat transfer inside solid structure are calculated in t_0-t_0+Δt.
4) The wall temperature solid domain at t_0+Δt is passed to the fluid domain as a new boundary condition for the flow field calculation

5) Repeat the calculation from step (2) to step (4) until all time steps are reached.
6) Upon completion of the bidirectional coupling interaction, a structural analysis is performed by means of pressure distributions in coupled surface and temperature field distributions in solid part, in order to evaluate the thermal response in terms of stresses, deformations and displacements.

3. Validation of numerical model

3.1. Validation of fluid-thermal-structural coupled analysis method

In order to verify reliability of the fluid-thermal-structural coupling method, a stainless steel cylindrical heating experiment[17] was used for comparison. The experiment was conducted in NASA Langley Center's 8 ft high temperature wind tunnel, and the free-stream Mach number is 6.47. The outer diameter of the tube was 38.1 mm and the inner diameter was 25.4 mm. In order to save computing resources, a three-dimensional 1/4 cylindrical model is adopted. The computational grid is shown in Fig 2. In fluid domain, the total number of grids is 600,000, and the grids are densely arranged near the shock and wall surfaces, which aims to predict aerodynamic heating accurately.

Fig 3 compares density of external flow field obtained from numerical simulation, and the schlieren figure of experiment. The position and shape of bow shock in the calculation results are in good agreement with the experiment results.

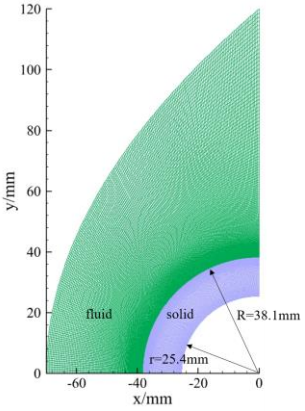

Fig 2. Grids of the cylindrical leading edge

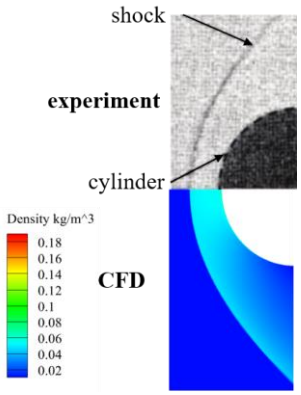

Fig 3. Results of computation in flow field

Fig 6 shows the comparison between the predicted and experimental values of cylindrical surface pressure, as P/P_0 is the ratio of wall pressure to stationary pressure, and θ is the central angle of the cylindrical model. The pressure distribution is in good agreement. The maximum pressure of flow field after the shock is 35380 Pa, which is 6.21% different from the experimental value. As shown in Fig 5, the temperature distribution of numerical simulation agrees well with the experimental results, and the experimental data points are located between the numerical curves at t = 4 s and t = 5 s. The computational reliability of the adopted coupling method is thus verified, so the fluid-thermal-structural coupling strategy can be introduced into the thermal analysis of hypersonic vehicles.

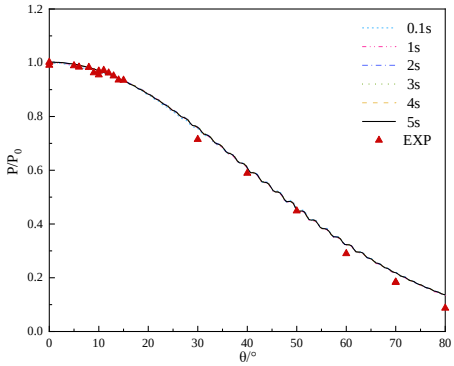

Fig 4. Comparison of surface pressure distribution

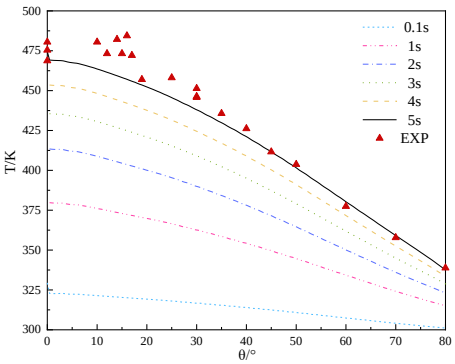

Fig 5. Comparison of surface temperature distribution

3.2. Validation of turbulence model

In this section, the experimental results of Hayashi[18] are selected to verify the applicability of the turbulence model on the opposing jet. The Mach number of experimental incoming flow is 3.98. The comparison of the density contour with the experimental schlieren figure is shown in Fig 6. The opposing jet generates an expansion wave at the nozzle, which interacts with the free incoming flow to form a stable and dense Mach disk, and the bow shock is pushed away by the jet and reaches the downstream of body surface to form a recompressed shock. The reasonable agreement is obtained with the computed and experimental flow structures. It indicates that the SST k-ω turbulence model is highly accurate in simulating the flow field of opposing jet, which is shown by the good agreement in the sizes and positions of the typical structures such as bow shock, Mach disk, recirculation region, and recompressed shock.

The dimensionless parameter Stanton number, St, is chosen to characterize the measure of heat flux at the wall of the blunt body. The St represents the ratio of heat transferred to the fluid to heat capacity of the fluid and is defined as follows：

$$St = \frac{q}{(T_{aw}-T_w)\rho_\infty C_{p\infty} u_\infty} \tag{1}$$

$$T_{aw} = T_\infty \left\{1 + \sqrt[3]{Pr}[\frac{(\gamma-1)}{2})Ma_\infty^2]\right\} \tag{2}$$

Fig 7 is the comparison of the St distribution on the surface between the numerical simulation data and the experimental data. The two results match well, which proves the accuracy of the simulation model. In the diagram, θ represents the direction of free flow and the radius vector from the center of curvature.

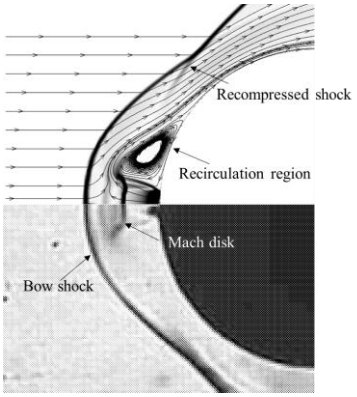

Fig 6. Density comparison between numerical and experimental data

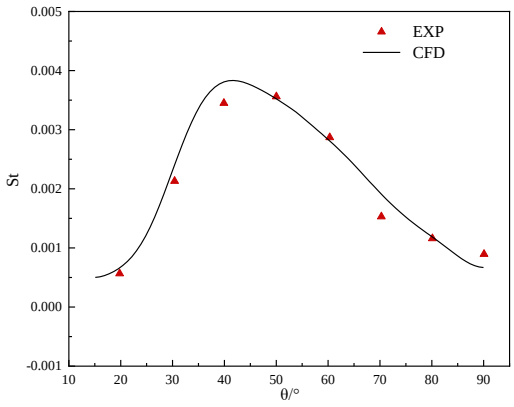

Fig 7. Stanton number comparison

4. Results and discussion

4.1. Feature of the flow field

In hypersonic incoming flow, a bow shock is generated at the leading edge of the air rudder, as shown in Fig 8, the pressure of the flow field after the bow shock increases sharply and the temperature has steep rise, which is especially obvious at the stationing point of the leading edge. The flow field in front of the stationary point forms a high-temperature and high-pressure region, and the intensity of the flow field heating and pressurization gradually decreases as the shock propagates downstream. It can be seen that the hypersonic flow brings serious aerodynamic drag and heat problems to the air rudder, so the technology of drag reduction and thermal protection is particularly critical.

The Ma, temperature, density and pressure distributions in flow field with porous opposing jet are shown in Fig 9. From the Ma and temperature contours, it can be seen that the introduction of the porous opposing jet causes flow field to reconfigure at the leading edge of the air rudder. The bow shock and the high temperature region are pushed outward by the opposing jet. The jet interacts with the incoming flow to form multiple Mach disk structures and contact surface. Multiple recirculation region is wrapped with the contact surface, and the temperature and Mach number of the recirculation

region decrease significantly. In addition, the thickness of the bow shock at the leading edge is no longer uniform under the influence of the opposing jet, but shows regular fluctuation.

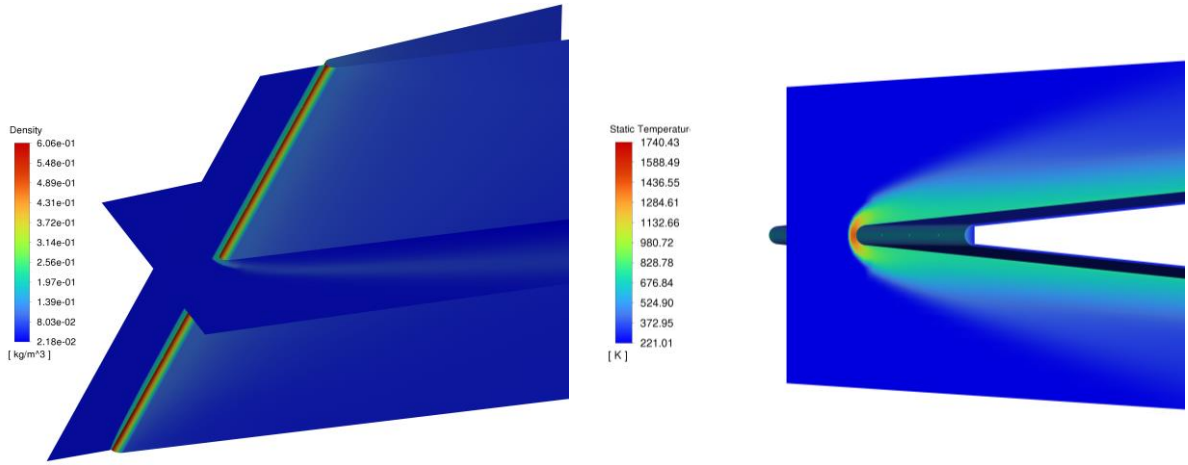

(a) density (b) Temperature

Fig 8. Flow field structure without opposing jet

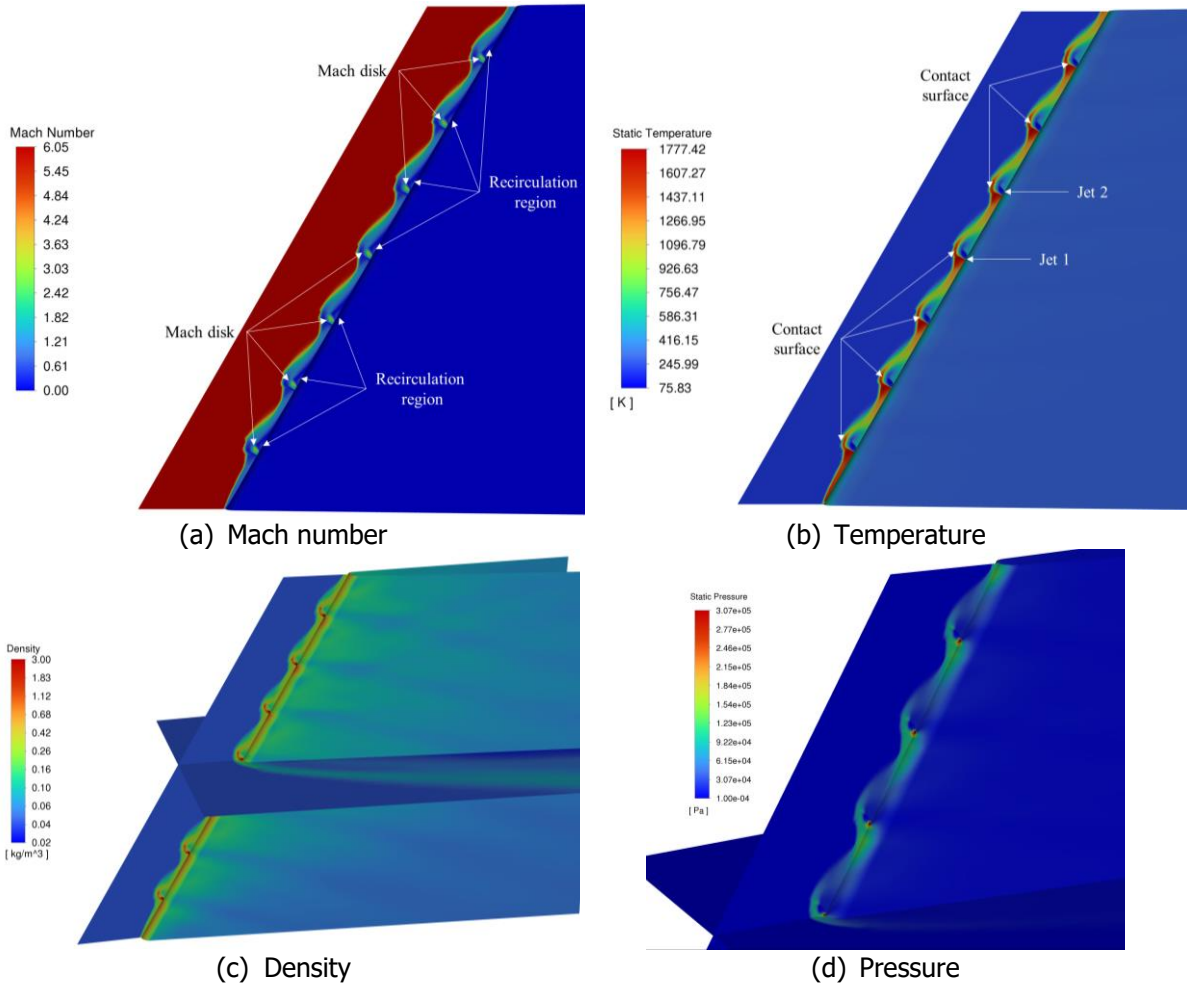

(a) Mach number (b) Temperature

(c) Density (d) Pressure

Fig 9. Flow field structure of the porous opposing jet

Take jet 1 and jet 2 as an example to analyze the interaction between the jet, as shown in Fig 10. It indicates that there is still a localized high-temperature and high-pressure region downstream of jet 2. There are two main reasons for this phenomenon. Firstly, the ejection direction of the opposing jet is perpendicular to the rudder, resulting in a certain angle between the jet and the hypersonic incoming flow, and by the action of the incoming flow, the jet is biased toward the upstream after ejection.

Secondly, the spacing of jet orifices is large. Jet 1 flows to both sides of the rudder surface through the leading edge after ejection, and its effect on jet 2 is weak. Obviously, the jet orifices spacing is one of the important factors affecting its drag and heat reduction performance. It is hoped that the adverse factor caused by the local high temperature and pressure area can be improved by adjusting the spacing of the jet orifices.

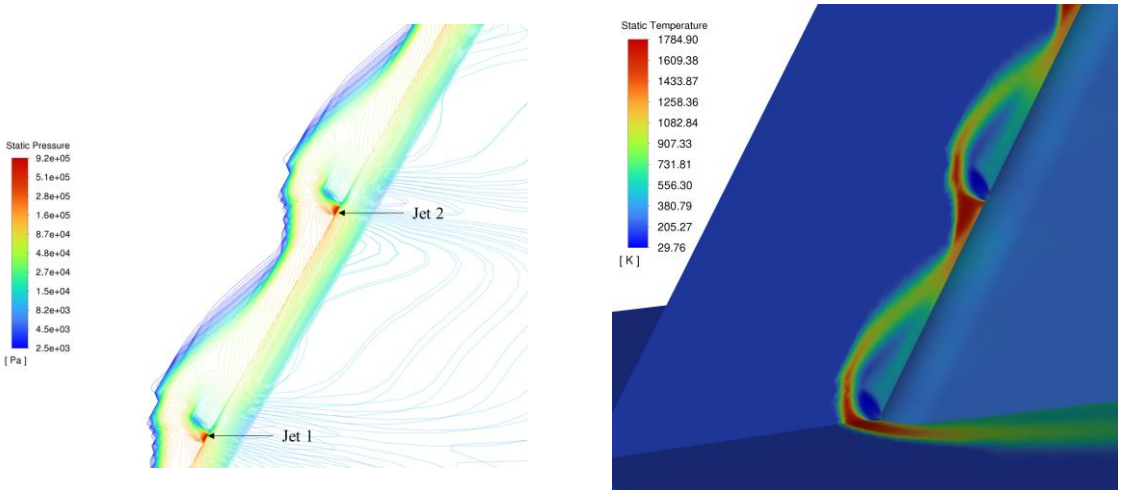

(a) Pressure (b) Temperature

Fig 10. Interaction between the jet

4.2. Response of thermal structure

Fig 11 shows the comparison of porous jet and no jet at t =0.5 s. By analyzing Line A, it is found that the patterns of wall pressure and temperature sectional drawing change inconsistently under the no jet and porous opposing jet schemes, which is due to the fact that the porous opposing jet changes the structure of the flow field. The pressure and temperature distributions at the leading edge in the absence of jet are more stable, which are around 1×10^5 Pa and 600 K in turn.

Combined with the contours, it can be seen that the peaks appearing in the pressure curves of the porous jet are caused by the jet ejection in opposing direction, while the wall pressure near jet holes is significantly reduced. Due to the jet injection angle, a certain high temperature region still exists downstream of the nozzle, but the overall wall temperature is significantly reduced by the cooling effect of the recirculation region.

On Line B, circumferentially around the rudder leading edge, the heat flux and wall temperature of the porous opposing jet scheme show a significant decrease compared to the no jet. The peak temperature without jet is 604 K, which occurs at the stationary point. The peak temperature with porous jet drops to 461 K, with an temperature reduction of about 20% and a heat flux reduction of 25%. Taken together, the porous opposing jet can provide good results in both drag reduction and thermal protection.

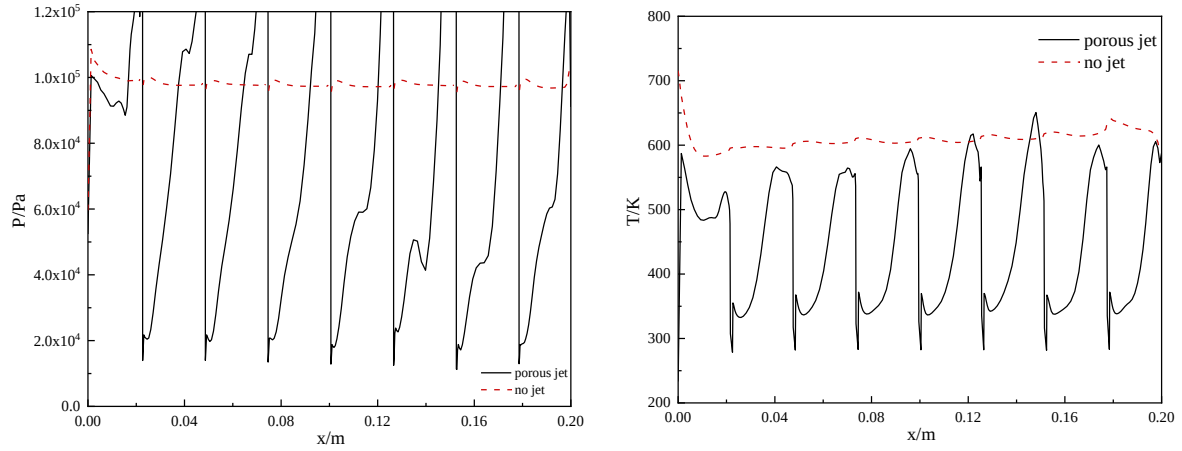

(a) pressure of Line A (b) temperature of line A

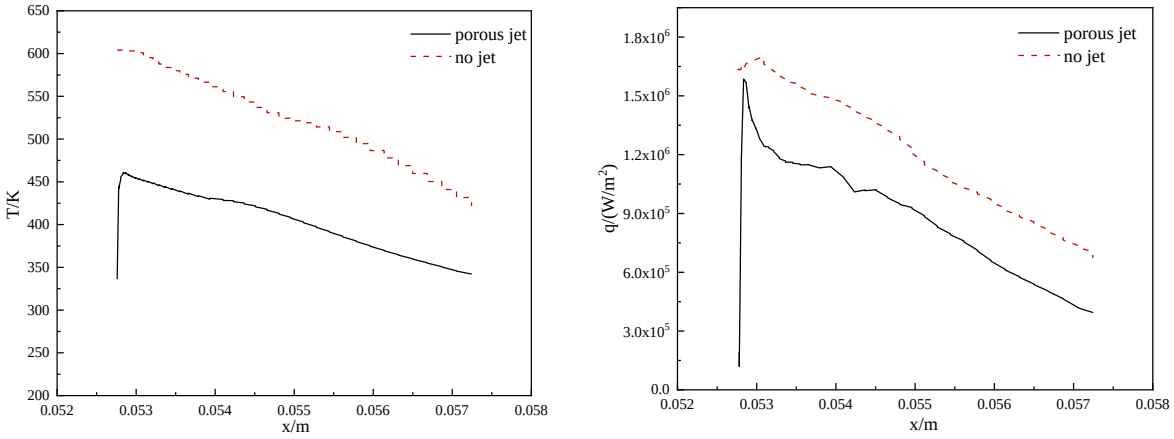

(c) temperature of Line B (d) heat flux of line B

Fig 11. Comparison of porous jet and no jet at t =0.5 s

From t =0 s to 40 s, the surface temperature distribution in leading edge is more uniform from the highest temperature point to both sides of the rudder. This is mainly due to the jet cooling effect, coupling process and heat conduction in the solid structure. The details of the solid temperature variations are presented in Fig 12, where the vertical section is y = 0 m, and starting from z = 0.1 m, horizontal sections are taken at 0.005m intervals, for a total of six. The temperature of structure near jet upstream is low, which is mainly caused by the cooling effect of low-temperature recirculation. In summary, the simulation of isothermal wall is not accurate enough for heat-flow prediction, and the fluid-thermal-structural coupling method is necessary for precise aerodynamic heat prediction.

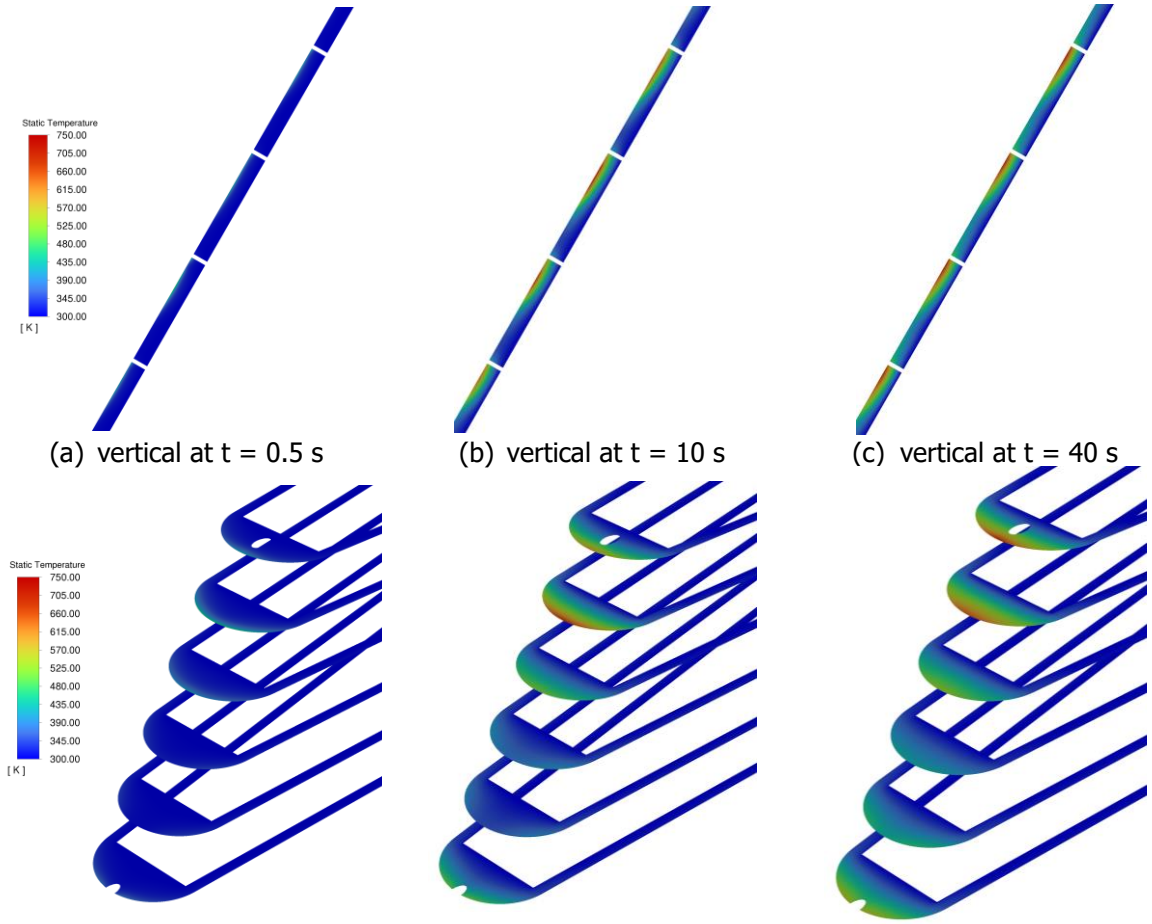

(a) vertical at t = 0.5 s (b) vertical at t = 10 s (c) vertical at t = 40 s

(d) horizontal at t = 0.5 s (e) horizontal at t = 10 s (f) horizontal at t = 40 s

Fig 12. Sectional drawing Contours of temperature

Fig 13 provides the temperature distribution in horizontal section. As time goes on, the peak temperature of centerline rises from 315 K to 473 K, which indicates the external aerodynamic heating gradually penetrates into the internal structure, and there is an obvious heat transfer phenomenon in the solid domain. The temperature field distribution and structural bearing changes in solid domain, which also affects the heat transfer at the fluid-solid interface.

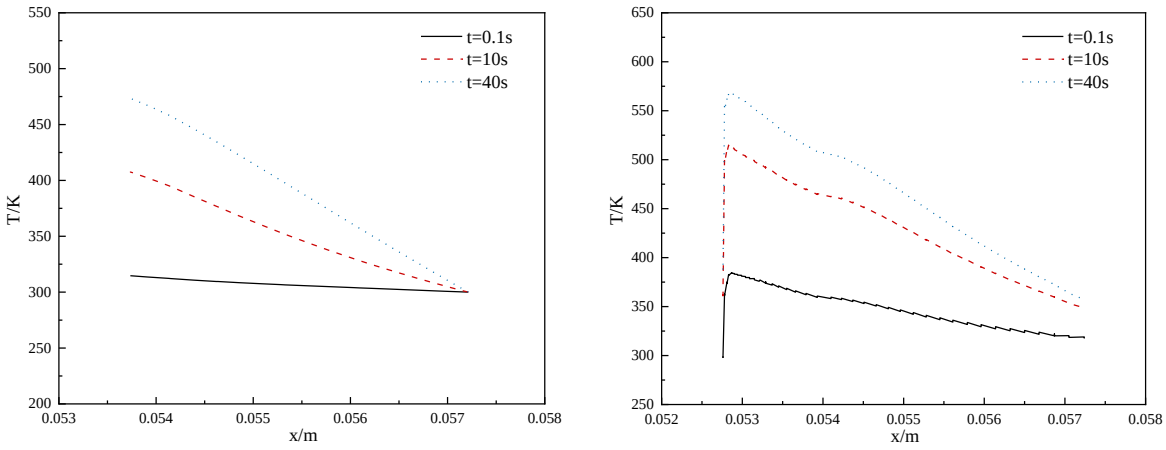

(a) centerline (b) line B

Fig 13. Temperature distribution in horizontal section

5. Conclusions

In order to study the drag reduction and thermal protection effect of the opposing jet configuration on the air rudder in hypersonic flight, numerical simulations of the flow and structural thermal response characteristics of the porous jet under Mach 6 free stream are carried out, by using the fluid-thermal-structural coupling strategy. The main conclusions are as follows:

1) The introduction of the porous opposing jet changes the flow field at the leading edge of the air rudder, the bow shock and the high temperature region at the leading edge are pushed outward by the opposing jet, *Ma* and temperature after the shock decrease significantly, and the shock surface shows regular undulations.
2) When the spacing of jet orifices is large, the interaction between the jet is weak. Therefore, the jet hole spacing and so on are important factors affecting the performance of drag and heat reduction, and it will be very meaningful to analyze and study their effects. In addition, there exists an optimal combination of structural parameters that makes the porous jet most effective in drag reduction and thermal protection.
3) The porous opposing jet can be effective in both drag reduction and thermal protection. The peak circumferential temperature at the leading edge decreases to 461 K by the cooling effect of the recirculation region, the overall temperature at the leading edge decreases by about 20%, and the heat flux decreases by about 25%.

References

1. Mcnamara J. J., Friedmann P. P.: Aeroelastic and Aerothermoelastic Analysis in Hypersonic Flow: Past, Present, and Future. AIAA JOURNAL. 49(6), 1089-122 (2011)
2. Ahmed M. Y. M., Qin N.: Forebody shock control devices for drag and aero-heating reduction: A comprehensive survey with a practical perspective. Progress in Aerospace Sciences. 112, 100585 (2020)
3. Wang Z.G., Sun X.W., Huang W., Li S.B., Yan L.: Experimental investigation on drag and heat flux reduction in supersonic/hypersonic flows: A survey. Acta Astronautica. 129, 95-110 (2016)
4. Sun X., Huang W., Ou M., Zhang R., Li S.: A survey on numerical simulations of drag and heat reduction mechanism in supersonic/hypersonic flows. Chinese Journal of Aeronautics.

32(4), 771-84 (2019)

5. Huang W.: A survey of drag and heat reduction in supersonic flows by a counterflowing jet and its combinations (Review). Journal of Zhejiang University: Science A. 16(7), 551-61 (2015)
6. Huang W., Chen Z., Yan L., Yan B. B., Du Z. B.: Drag and heat flux reduction mechanism induced by the spike and its combinations in supersonic flows: A review. Progress in Aerospace Sciences. 105, 31-9 (2019)
7. Fan W.-J., Li S.B., Zhou J., Huang W., Ou M., Zhang R.-R.: Study on the drag and heat reduction performance of porous opposing jet in hypersonic flow. International Journal of Heat and Mass Transfer. 139, 351-61 (2019)
8. Li S.B., Zhang T.T., Ou C., Huang W., Chen J.: Mechanism study on drag reduction and thermal protection for the porous opposing jet in hypersonic flow. Aerospace Science and Technology. 103, 105933 (2020)
9. Li S.B., Huang W., Lei J., Wang Z.G.: Drag and heat reduction mechanism of the porous opposing jet for variable blunt hypersonic vehicles. International Journal of Heat And Mass Transfer. 126, 1087-98 (2018)
10. Liu H. P., Wang Z. G., Ding M.: Fluid-thermal coupled analysis of heat reduction by the opposing jet in hypersonic flows. International Journal of Heat and Mass Transfer. 147, 119003 (2020)
11. Liu H. P., Wang Z. G.: Fluid-thermal-structural coupling investigations of opposing jet in hypersonic flows. International Communications in Heat and Mass Transfer. 120, 105017 (2021)
12. Meng Y. S., Wang Z. W., Huang W., Niu Y. B., Yan L.: Coupled fluid-thermal analysis of the reduction mechanism for the drag and heat flux induced by jet interaction in a hypersonic reusable launch vehicle. AIP Advances. 12, 105124 (2022)
13. Zhu L., Li Y., Chen X., Li H., Li W., Li C.: Hypersonic flow characteristics and relevant structure thermal response induced by the novel combined spike-aerodome and lateral jet strategy. Aerospace Science and Technology. 95, 105459 (2019)
14. Meng Y.S., Yan L., Huang W., Wang Z.W.: Fluid-thermal coupled investigation on the combinational spike and opposing/lateral jet in hypersonic flows. Acta Astronautica. 185, 264-82 (2021)
15. Meng Y. S., Yan L., Huang W., Ji C., Li J.: Coupled investigation on drag reduction and thermal protection mechanism of a double-cone missile by the combined spike and multi-jet. Aerospace Science and Technology. 115, 106840 (2021)
16. Meng Y. S., Yan L., Huang W., Zhao Z. T.: Coupled investigation on drag and heat flux reduction over spiked waverider with a wide-speed range Acta Astronautica 182, 498-516 (2021)
17. Wieting A.: Experimental study of shock wave interference heating on a cylindrical leading edge. Virginia, Old Dominion University (1987)
18. Hayashi K., Aso S., Tani Y.: Experimental Study on Thermal Protection System by Opposing Jet in Supersonic Flow. Journal of Spacecraft and Rockets. 43(1), 233-5 (2006)